FERMILAB-PUB-09-322-APC

Transverse Modes of a Bunched Beam at Space Charge Dominated Impedance

V.Balbekov

Fermi National Accelerator Laboratory

P.O. Box 500, Batavia, Illinois 60510

June 24, 2009

Abstract

Coherent transverse oscillations of a bunched beam are considered at space charge dominated impedance and synchrotron motion taken into account. General equation for the bunch eigenmodes is derived, its exact analytical solution is found for a boxcar bunch at linear synchrotron oscillations, and numerical solutions are presented for other distributions. Both low and high synchrotron frequency approaches are considered and compared, fields of their application are established, and some estimations are proposed for the intermediate region.

1 Introduction

Transverse instability of a bunched beam with synchrotron oscillations taken into account was considerer first by C. Pellegrini [1] and M. Sands [2]. Coherent oscillations of the bunches were presented as a sum of uncoupled modes $\propto \exp(im\phi)$ where ϕ is synchrotron phase. After that, F. Sacherer [3] investigated this effect in more depth including so called radial modes describing dependence of the particles displacement on synchrotron amplitude.

Space charge effects were not taken into account in these works. It has been made first in paper [4] where space charge dominated impedance was

considered. It was shown that most of the bunch modes become stable due to Landau damping which is enhanced because of an additional tune spread produced by the space charge. The only mode which never prone to this kind of the damping is so called rigid mode.

However, this conclusion was made at the assumption that the space charge tune shift is small in comparison with synchrotron frequency – the condition which is violated very often. Some simple models (air-bag, square potential well) were examined later in paper [5] without these restrictions.

Low synchrotron frequency limit was considered recently in Ref. [6] at arbitrary distribution. However, most of presented there results are erroneous, first of all because of using of mathematically incorrect expressions like

$$\int_{-\infty}^{0} \exp(-i\Psi)\Psi \, d\Psi = 1, \qquad \text{etc.}$$

(some relevant details are commented in the text below).

In presented work, the problem is investigated at any distribution, both at small and large relation of tune shift to synchrotron frequency. However, expected instability growth rate is assumed to be enough small in all the cases:

$$\operatorname{Im}\omega \ll \Omega_s, \qquad \operatorname{Im}\omega \ll \Omega_0 \Delta Q$$

where Ω_s and Ω_0 are synchrotron and revolution frequencies, ΔQ is betatron tune shift. The assumption allows to solve the problem in 2 stages: (i) determination of the bunch eigenmodes with space charge only; (ii) and investigation of their instability produced by additional wake field. The first point is considered in detail in presented work including the items:

- integral-differential equation of the eigenmodes is derived;
- its exact analytical solution for a boxcar bunch is first obtained and applied further to test different particular models;
- approximate differential equation is developed at low synchrotron frequency, and its analytical or numerical solutions are presented at different distribution functions;
- the same distributions are investigated in opposite case of high synchrotron frequency using uncoupled multipole model;
- applicability of different models is discussed by comparison of these ultimate cases.

It is presumed that bare (without space charge) betatron and synchrotron oscillation are linear. There are strong grounds to believe that their nonlinearity would enhance the Landau damping.

2 Basic equation for eigenmodes

We will start from equation of betatron oscillations of single particle:

$$\frac{d^2x}{dt^2} + \Omega^2 Q^2 x = \frac{eE\Big(\theta, x - \overline{X}(t,\theta), y\Big)}{m\gamma^3} + \frac{eG(t,\theta)}{m\gamma} \tag{1}$$

where Ω and Q are momentum-dependent angular velocity and tune, E is space charge electric field, and eG is Lorenz force per particle due to all other sources (resistive wall, cavities, etc.). In the beginning, we will neglect this part to find eigenfunctions (e.f.) and eigenvalues (e.v.) of the problem at $G \ll E/\gamma^2$. It should be taken into account later as a small perturbation to get additions to the e.v., including the instability growth rate.

The field E depends on the particle deviation from the bunch center: longitudinal θ and transverse $x - \overline{X}(t,\theta)$ where $\overline{X}(t,\theta)$ is the beam offset at azimuth θ (y-offset is presumed to be 0). Averaging Eq. (1) over all particles near point (θ, u) of longitudinal phase space, obtain equation for the function $X(t,\theta,u)$ which is a local displacement of the beam in this point:

$$\frac{d^2X}{dt^2} + \Omega^2 Q^2 X = \frac{e}{m\gamma^3} \int\limits_{-\infty}^{\infty} E(\theta, x + X - \overline{X}, y)\, \rho_\perp(x,y)\, dxdy. \tag{2}$$

where $\rho_\perp(x,y)$ is normalized steady-state beam density. Because both X and $\overline{X}$ are small in comparison with the beam diameter, it is possible to expand E in Taylor series resulting in

$$\frac{d^2X}{dt^2} + \Omega^2 Q^2 X = 2\Omega^2 Q \Delta Q(\theta)\, (X - \overline{X}) \tag{3}$$

where $\Delta Q(\theta)$ is the space charge driven tune shift at azimuth θ averaged over transverse coordinates:

$$\Delta Q(\theta) = \frac{e}{2m\gamma^3\Omega^2 Q} \int\limits_{-\infty}^{\infty} \frac{\partial E}{\partial x}(\theta, x, y) \rho_\perp(x,y)\, dxdy. \tag{4}$$

(it is taken into account that $\rho_\perp$ and E are even and odd functions of x). For an elliptical beam of constant density, ΔQ coincides with usual incoherent tune shift. For Gaussian beam, ΔQ is a half of tune shift of small oscillations. Other details can be found in Ref. [8].

Because $\Delta Q \ll Q$, Eq. (3) can be replaced by first order equation:

$$\frac{dX}{dt} + i\,\Omega\,QX \simeq i\,\Omega\Delta Q\,(X - \overline{X}). \tag{5}$$

Also, it is necessary to take into account that d/dt is actually total derivative over time including longitudinal motion:

$$\frac{d}{dt} = \frac{\partial}{\partial t} + \frac{d\theta}{dt}\frac{\partial}{\partial\theta} + \frac{du}{dt}\frac{\partial}{\partial u} = \frac{\partial}{\partial t} + \Omega_s\frac{\partial}{\partial\phi} \tag{6}$$

where $u \propto p$ is normalized momentum, ϕ and Ω_s are phase and frequency of synchrotron oscillations. We will look for solutions of obtained equation in the form:

$$X(t,\theta,u) = Y(\theta,u)\exp\Big(-i\omega t - i(Q_0 - \xi/\eta)\,\theta\Big) \tag{7}$$

where $\xi = dQ/d(\ln p)$ and $\eta = -d(\ln\Omega)/d(\ln p)$ are chromaticity and slippage factor, and subindex '0' marks central momentum. It allows to exclude dependence of Ω and Q on momentum in Eq. (5) resulting in:

$$(\omega - \Omega_0 Q_0)Y + i\,\Omega_s\frac{\partial Y}{\partial\phi} = -\Omega_0\Delta Q(\theta)\,(Y - \overline{Y}). \tag{8}$$

Further we will use the notations

$$\frac{\omega - \Omega_0 Q_0}{\Omega_0\Delta Q(0)} = \nu, \qquad \frac{\Omega_s}{\Omega_0\Delta Q(0)} = \mu \tag{9}$$

to represent Eq. (8) in the form:

$$\nu\,Y + i\,\mu\,\frac{\partial Y}{\partial\phi} = -\frac{\rho(\theta)}{\rho(0)}\,(Y - \overline{Y}). \tag{10}$$

where $\rho(\theta)$ is linear bunch density at longitudinal distribution function F:

$$\rho(\theta) = \int\limits_{-\infty}^{\infty} F(\theta,u)\,du. \tag{11}$$

Eq. (10) should be supplemented by relation of the variables $Y - \overline{Y}$:

$$\rho(\theta)\,\overline{Y}(\theta) = \int\limits_{-\infty}^{\infty} F(\theta,u)\,Y(\theta,u)\,du \tag{12}$$

which is valid for $X - \overline{X}$ pair as well. The equation was derived first in Ref. [4] with help of Vlasov equation in terms of function $D = FY$ which is linear density of the beam dipole moment. The transformation is trivial, but form (10) is used in this paper as more convenient.

Parameter ν can be treated as an eigenvalue of the equation. It is easy to show that all the e.v. are real numbers, and corresponding e.f. satisfy the orthogonality condition:

$$\int\int Y_i Y_j^* F d\theta du = \delta_{ij}, \qquad \mathrm{Im}\,\nu = 0. \tag{13}$$

Note one important exact solution which is valid at any distribution and will be treated further as a rigid mode [1] :

$$Y = \overline{Y} = const, \qquad \nu = 0, \quad \text{i.e.} \quad \omega = \Omega_0 Q_0 \tag{14}$$

Because of the orthogonality, all other solutions should satisfy the condition

$$\int\int Y_i F d\theta du = \int \overline{Y}_i(\theta)\rho(\theta)\,d\theta = \int \overline{D}_i(\theta)\,d\theta = 0. \tag{15}$$

which means that total dipole moment of the bunch is zero (at zero chromaticity). It is easy to believe that wake field of such a bunch and attendant instability (if appears) should be noticeably lower then for the rigid mode.

Further we will consider linear synchrotron oscillations taking the bunch half-length as 1:

$$\theta = A\cos\phi, \qquad u = A\sin\phi, \qquad A \le 1. \tag{16}$$

where $A = \sqrt{\theta^2 + u^2}$ is amplitude of synchrotron oscillations. Their nonlinearity is not considered in this paper because its contribution to Landau damping is presumed to be small in comparison with space charge effects.

[1] This term was originally used for the model without synchrotron oscillations, see for example Ref. [7]. We are applying it here because solution (14) just does not depend at all on synchrotron motion.

In conclusion of this section, it is important to note that the substitution $X \propto \exp(-i\omega t)$ in Eq. (7) means, strictly saying, Laplace transformation in time which is determined at $\mathrm{Im}\,\omega > 0$. It means that originally $\mathrm{Im}\,\nu > 0$ in Eq. (10), too. Therefore, any real e.v. of this equation has a direct sense only if corresponding e.f. is a regular function defined as analytical extension of the primary complex functions on real axis. Otherwise, it is necessary to bypass the pole at inverse Laplace transformation, which operation provides Landau damping [9].

Therefore, only regular solutions of Eq. (10) have a chance to become unstable due to the addition $\propto G$ in Eq. (1) (for example, rigid mode). Other (irregular) modes are prone to the Landau damping, and only strong perturbation G could cause their instability by an essential transformation of original spectrum; however, similar situation is not a subject of this work. For shortness, we will below identify mentioned modes simply as "unstable" or "stable" ones.

3 Boxcar bunch: exact solution

A bunch of constant linear density is considered in this section:

$$F = \frac{1}{\pi\sqrt{1-\theta^2-u^2}}, \qquad \rho = 1 \quad \text{at} \quad |\theta| < 1. \tag{17}$$

Such a distribution was investigated numerically in Ref. [5]. In fact, Eq. (10) has an exact and full analytical solution at any μ in this case, offering an excellent prospect to check any approximate model in further. The solution is set of Legendre polynomials:

$$\overline{Y}(\theta) \propto P_n(\theta), \qquad n = 0,\, 1,\, 2, ... \tag{18}$$

In each the case, there are $n+1$ different e.v. ν and corresponding e.f. $Y(\theta, u)$ which are polynomials of the same power, too. Several examples are given below:

n=0 $\qquad \overline{Y} = Y = 1, \qquad \nu = 0, \qquad$ (rigid mode);

n=1 $\qquad \overline{Y} = \theta, \qquad Y = \theta + \dfrac{i\,\nu u}{\mu}, \qquad \nu = -\dfrac{1}{2} \pm \sqrt{\mu^2 + \dfrac{1}{4}};$

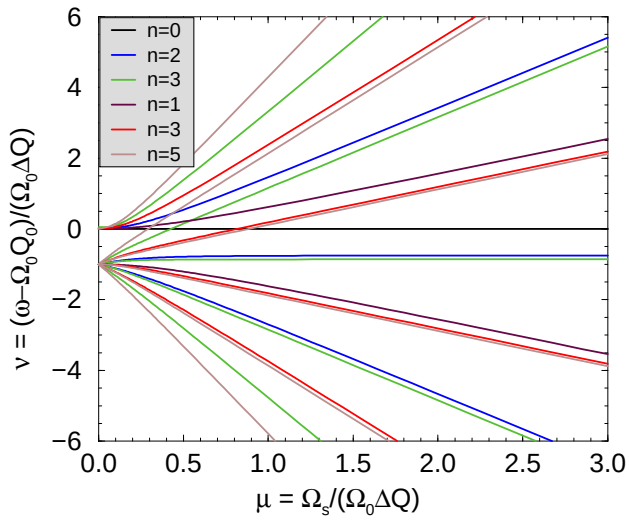

Figure 1: Exact eigenvalues of boxcar bunch.

n=2 $\qquad \overline{Y} = 3\theta^2 - 1, \qquad \hat{\nu}(\hat{\nu}^2 - 4\mu^2) = \hat{\nu}^2 - \mu^2, \qquad \hat{\nu} = \nu + 1;$

n=3 $\qquad \overline{Y} = 5\theta^3 - 3\theta, \qquad (\hat{\nu}^2 - \mu^2)(\hat{\nu}^2 - 9\mu^2) = \hat{\nu}(\hat{\nu}^2 - 4\mu^2).$

Continuation of the table is very apparent. The eigenvalues ν are plotted in Fig. 1 vs μ at $n = 0 - 5$. It is seen that, at large μ, some eigenmodes form groups with rather close frequencies and about circular polarization:

$$Y_{m,n} \simeq R_{m,n}(A)\exp(im\phi), \qquad \nu \simeq \pm m\mu, \qquad \omega \simeq \Omega_0 Q_0 \pm m\Omega_s.$$

which coincide with well-known head-tail modes [1, 2, 3]. It is seen also that radial modes $R_{m,n}(A)$ arise here from different Legendre polynomials $P_n(\theta)$.

At lower μ, any e.v. tends to one of two points: $\nu \simeq 0$ or $\nu \simeq -1$. In usual terms, frequencies of these oscillations are:

$$\omega \simeq \Omega_0 Q_0 \qquad \text{or} \qquad \Omega \simeq \Omega_0(Q_0 - \Delta Q) = \Omega_0 Q_{incoherent}.$$

These oscillations are almost linearly polarized: along θ in first case, and along u in second one. Because of the frequencies coalescing, there is almost total degeneration of corresponding e.f. at $\mu \ll 1$. In particular, the following formal solutions can be obtained directly from Eq. (10) at $\mu = 0$:

$$\begin{array}{llllll} \text{any} & Y(\theta) & \text{and} & \overline{Y} = Y & \text{at} & \nu = 0; \\ \text{any} & Y(\theta, u) & \text{but} & \overline{Y} = 0 & \text{at} & \nu = -1. \end{array}$$

(second case at $\rho = const$ only). Of course, these sets cannot provide a basis for further investigations. However, at very realistic conditions $\mathrm{Im}\,\omega \ll \Omega_s$, synchrotron motion could remove the degeneration and form the modes available for subsequent generalization.

Our nearest goal is to use these ideas for analysis of more realistic distributions at $\mu \ll 1$. The case $\nu \simeq 0$ is rather clear offering an expansion of the solutions in powers of u. Other case $\nu \simeq -1$ is more complicated because the condition $\rho(\theta) = const$ is crucial for them ensuring a constant incoherent frequency. As this take place, different parts of the bunch can oscillate with the same frequency, creating various spatial configurations. However, only a short part of the bunch can have a definite incoherent frequency at $\rho(\theta) \neq const$. Then the term $\mu\, \partial Y/\partial\phi$ looks about as $0 \times \infty$, and cannot be treated as a small perturbation of Eq. (10).

However, instability of similar oscillations looks unlikely because: (i) Landau damping works when coherent frequency is located inside incoherent distribution, (ii) actually, relation $\overline{Y} \simeq 0$ means low wake field. Therefore, in next section we will consider only the first case, looking for approximate solution of Eq. (10) by its expansion in powers of u at $|\mu \partial Y/\partial\phi| \ll 1$ and $\nu \propto \mu^2 \ll 1$.

4 Low synchrotron frequency approach

We will look for solution of Eq. (10) at $\mu \ll 1$ in the form:

$$Y = y_0(\theta) + y_1(\theta)u + y_2(\theta)u^2, \qquad |y_0| \gg |y_1| \gg |y_2|. \tag{19}$$

Then according to Eq. (12)

$$\overline{Y}(\theta) = \frac{\rho(\theta)}{\rho(0)} \left[y_0(\theta) + y_2(\theta) U^2(\theta) \right] \tag{20}$$

where

$$U^2(\theta) = \frac{\int F(\theta, u) u^2 du}{\int F(\theta, u) du}. \tag{21}$$

Substituting it into Eq. (10) and neglecting the terms μy_2 obtain

$$\nu(y_0+y_1u+y_2u^2)+i\mu(-y_0'u-y_1'u^2+y_1\theta) \simeq -\frac{\rho}{\rho(0)}\left[y_1u+y_2(u^2-U^2)\right] \quad (22)$$

where prime means derivative on θ. It gives the relations

$$y_1 = \frac{i\mu y_0'}{\nu+\rho/\rho(0)}, \qquad y_2 = -\frac{\mu^2}{\nu+\rho/\rho(0)}\left(\frac{y_0'}{\nu+\rho/\rho(0)}\right)', \quad (23)$$

and differential equation for y_0:

$$\nu y_0 = \frac{\mu^2}{\nu+\rho/\rho(0)}\left[y_0'\theta - \frac{\rho U^2}{\rho(0)}\left(\frac{y_0'}{\nu+\rho/\rho(0)}\right)'\right]. \quad (24)$$

Using Eq. (20) and (22), one can represent y_0 in terms of $\overline{Y}$. At the same accuracy as before, the relation is

$$y_0 \simeq \overline{Y} + \frac{\mu^2U^2}{\nu+\rho/\rho(0)}\left(\frac{\overline{Y}'}{\nu+\rho/\rho(0)}\right)'. \quad (25)$$

Substitution of this to Eq. (24) results in the equation:

$$U^2\overline{Y}'' - \left(\theta + \frac{U^2\rho'/\rho(0)}{\nu+\rho/\rho(0)}\right)\overline{Y}' + \frac{\nu(\nu+\rho/\rho(0))}{\mu^2}\overline{Y} = 0. \quad (26)$$

Because it has a solution at any ν, additional conditions are required to select the satisfying basic Eq. (10). First of all, it is the rigid mode $\nu = 0$, $\overline{Y} = 1$. All other modes should satisfy orthogonality condition (15) which is sufficient for even functions $\overline{Y}(\theta)$. For odd ones, multiply Eq. (10) on $F\theta$ and integrate it over $d\theta du$. Then, applying Eq. (19), (23), and (25) with accepted accuracy, one can get required condition [2]

$$\int \overline{Y}(\theta)\rho(\theta)\theta\, d\theta \simeq \frac{\mu^2}{\nu}\int \frac{U^2(\theta)\overline{Y}'(\theta)\rho(\theta)\, d\theta}{\nu+\rho(\theta)/\rho(0)}. \quad (27)$$

[2]Following equation is proposed in Ref. [6] instead of Eq. (26), (15), (27):

$$\nu\overline{Y} + \Delta Q(0)\,\mu^2U(\theta)\sqrt{\rho(\theta)}\frac{d}{d\theta}\left(\frac{U(\theta)}{\sqrt{\rho(\theta)}}\frac{d\overline{Y}}{d\theta}\right) = 0, \qquad \frac{d\overline{Y}(\pm\infty)}{d\theta} = 0.$$

Errors of the development were noted in Section 1. Some additional comments are: (1) factor $\Delta Q(0)$ here is incompatible with Eq. (10); (2) at the boxcar bunch, Legendre polynomials of Sec. 3 do not satisfy this equation, (3) boundary conditions imposed beyond the bunch boundaries look at least affectedly; (4) they are certainly inapplicable to the Legendre polynomials.

4.1 Boxcar bunch

Boxcar bunch (17) is considered in this subsection again:

$$\rho(\theta) = 1, \qquad U^2(\theta) = \frac{1-\theta^2}{2} \quad \text{at} \quad |\theta| < 1 \tag{28}$$

Then Eq. (26) transforms to Legendre equation:

$$(1-\theta^2)\overline{Y}'' - 2\theta\,\overline{Y}' + \frac{2\nu(\nu+1)}{\mu^2}\,\overline{Y} = 0. \tag{29}$$

Legendre polynomials (18) are the solutions satisfying conditions (15) and (27), and dispersion equation for corresponding e.v. is

$$\frac{2\nu(\nu+1)}{\mu^2} = n(n+1), \qquad \text{at} \qquad \overline{Y}(\theta) = P_n(\theta). \tag{30}$$

Taking into account the basic assumptions of this section, we must use the only eigenvalue:

$$\nu = \frac{1}{2}\Big(\sqrt{1+2\mu^2 n(n+1)} - 1\Big) \simeq \frac{\mu^2 n(n+1)}{2} \tag{31}$$

which is in total agreement with results of Sec. 3.

4.2 Parabolic bunch

More realistic parabolic bunch has the characteristics:

$$F = \frac{2}{\pi}\sqrt{1-A^2}, \qquad \rho = 1-\theta^2, \qquad U^2 = \frac{1-\theta^2}{4}. \tag{32}$$

Some its e.f. and corresponding e.v. are plotted in Fig. 2. The e.v. do not very differ from the boxcar ones, Eq. (31). However, it is important to note that the eigenfunctions depend on parameter μ now, and there is a growth of these functions at the bunch tails when the parameter is more. [3]

[3] Of course, it is not quite legitimately to consider the case $\mu \sim 1$ in this section. However, it will be shown soon that such an assumption does not lead to qualitative errors.

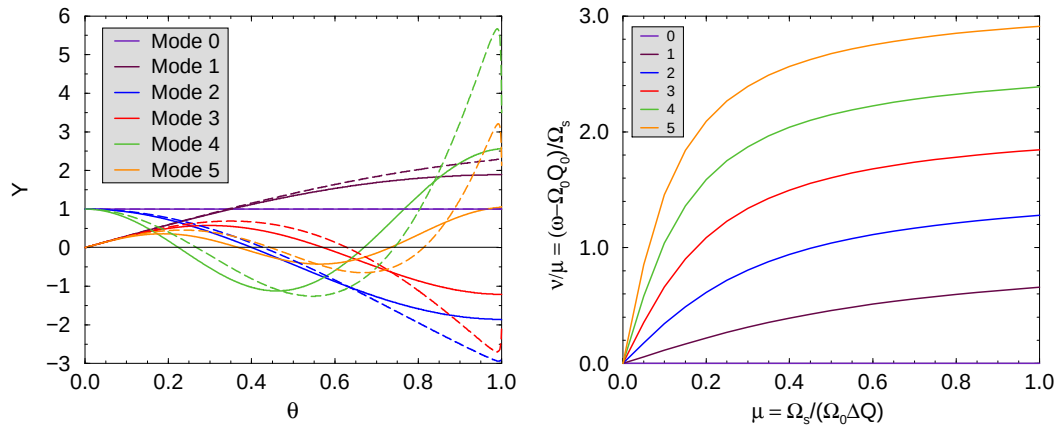

Figure 2: Eigenfunctions (left) and eigenvalues (right) of parabolic bunch. In the left-hand plot: solid lines $\mu = 0.05$, dashed ones $\mu = 1$.

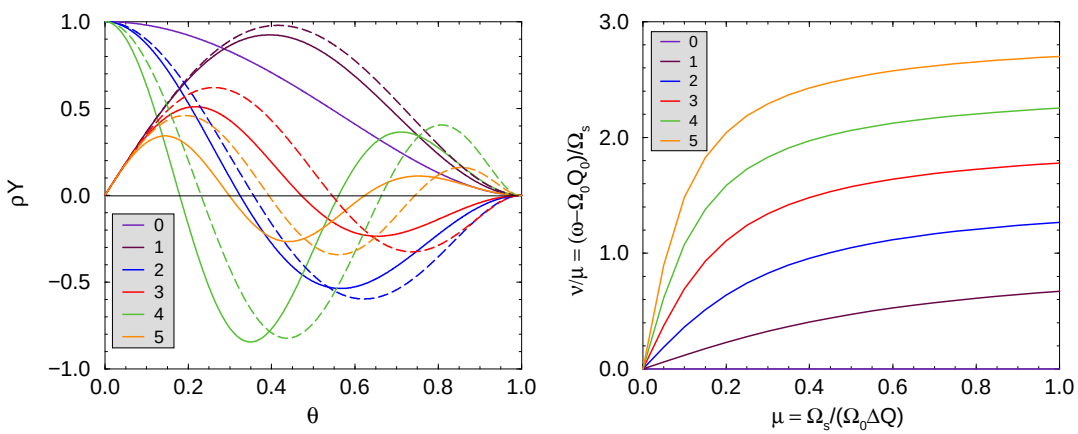

Figure 3: Eigenfunctions (left) and eigenvalues (right) of "super-parabolic" bunch. In the left-hand plot: solid lines $\mu = 0.05$, dashed ones $\mu = 1$.

4.3 "Super-parabolic" bunch

Distribution function (32) has infinite derivative on the boundary which circumstance could qualitatively effect on the results. Therefore, more smooth distribution is considered in this subsection:

$$F = \frac{8}{3\pi}(1 - A^2)^{3/2}, \qquad \rho = (1 - \theta^2)^2, \qquad U^2 = \frac{1 - \theta^2}{6}. \tag{33}$$

The results are presented in Fig. 3. In this case, all the eigenfunctions $\overline{Y}(\theta)$ demonstrate very fast growth in the bunch tails, especially at large μ (except the rigid mode). Therefore, the bunch dipole moment $D = \rho\overline{Y}$ is plotted vs θ in the left-hand plot instead of $\overline{Y}$ (including the rigid mode). [4]

4.4 Gaussian bunch

Because Gaussian bunch is always truncated in reality, we will consider the distribution function:

$$F \propto \exp\Big(\frac{1-A^2}{2\sigma^2}\Big) - 1 \qquad \text{at} \qquad A < 1 \tag{34}$$

which provides a bounded bunch with smooth tails at $|\theta| < 1$:

$$\rho(\theta) = \sigma\sqrt{\frac{\pi}{2}}\,\exp\Big(\frac{1-\theta^2}{2\sigma^2}\Big)\,\mathrm{erf}\Big(\frac{\sqrt{1-\theta^2}}{\sigma\sqrt{2}}\Big) - \sqrt{1-\theta^2}, \tag{35}$$

$$\rho'(\theta) = -\frac{\theta}{\sigma^2}\Big[\rho(\theta) + \sqrt{1-\theta^2}\Big], \qquad U^2(\theta) = \sigma^2 - \frac{(1-\theta^2)^{3/2}}{3\rho(\theta)}. \tag{36}$$

Results are presented in Fig. 4 at $\sigma = 1/3$ and $0 < \mu < 0.2$, where e.v. are scaled in accordance with Eq. (31). It is seen that the eigenfunctions tend to constant on the bunch tails at small μ, but they rapidly grow at $\mu = 0.2$. Very large (infinite?) divergence appears at more μ; therefore, density of the dipole moment $D = \rho\overline{Y}$ is presented in Fig. 5 at $0 \le \mu \le 1$.

4.5 Low μ summary

At $\mu = \Omega_s/\Omega_0\Delta Q <\sim 0.1$, all observed e.f. are finite and regular functions, and e.v. are not very different from the boxcar case. However, transverse deviation heavily increases at the bunch tails at more μ, maybe even infinitely at $\mu \sim 1$. It could mean that Eq. (26) has no regular ("unstable") solutions in this limit, except the rigid mode. Because this equation was initially developed at assumption $\mu \ll 1$, the last statement needs more support.

[4] Possibly, $\overline{Y}(\theta) \to \infty$ at $\theta \to 1$ and $\mu \sim 1$. Numerical accuracy gives no way to make a high-reliability conclusion, because growth of the functions is always restricted at similar calculations.

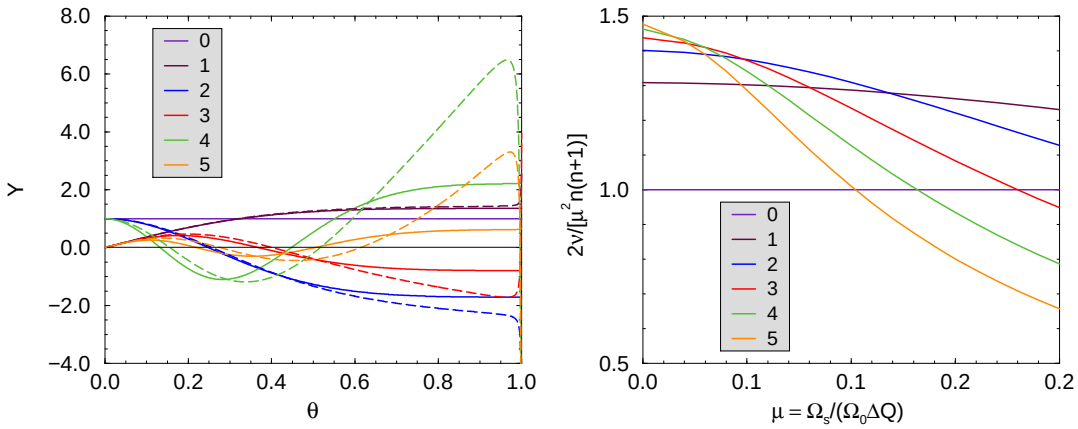

Figure 4: Eigenfunctions (left) and eigenvalues (right) of Gaussian bunch at $\sigma = 1/3$ and low μ. In the left-hand plot: solid lines $\mu = 0.01$, dashed ones $\mu = 0.2$.

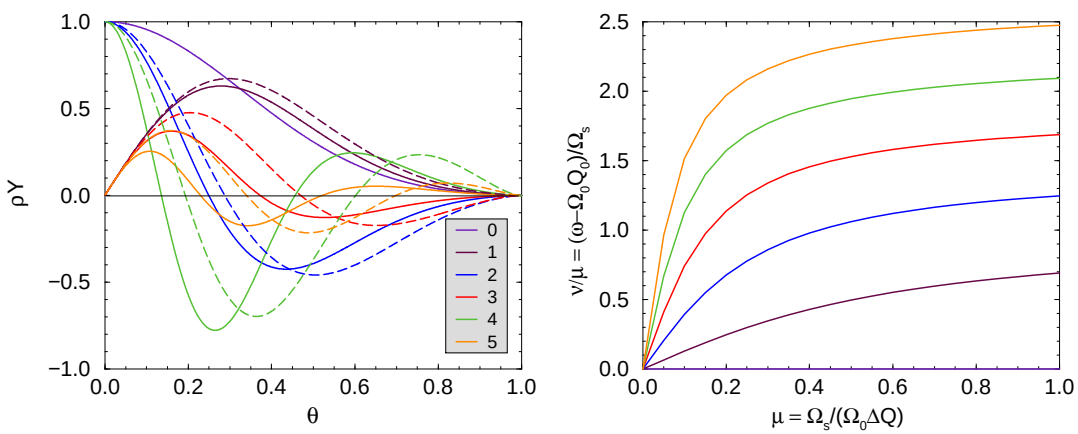

Figure 5: Eigenfunctions (left) and eigenvalues (right) of Gaussian bunch at higher μ. In the left-hand plot: solid lines $\mu = 0.05$, dashed ones $\mu = 1$.

Therefore, opposite limit $\mu \gg 1$ is considered in following section using an approximation of uncoupled multipoles. Though this case was investigated earlier in my work [4], an additional information is presented here having a final goal to develop an entire picture – at least qualitatively.

5 High synchrotron frequency approach

Because Y is a periodical function of ϕ, it can be presented in the form:

$$Y = \sum_m Y_m(A) \exp(im\phi). \tag{37}$$

Its substitution to integral-differential Eq. (10) results in series of integral equations:

$$(\nu - m\mu) Y_m(A) = -\sum_{m'} R_{m-m'}(A) Y_{m'}(A) + \sum_{m'} \int_0^\infty K_{m,m'}(A, A') Y_{m'}(A')\, dA'$$

with coefficients (38)

$$R_{m-m'}(A) = \frac{1}{\pi\rho_0} \int \frac{T_{m-m'}(\theta/A)}{\sqrt{A^2 - \theta^2}}\, \rho(\theta)\, d\theta, \tag{39}$$

$$K_{m,m'}(A, A') = \frac{2F(A')A'}{\pi\rho_0} \int \frac{T_m(\theta/A)}{\sqrt{A^2 - \theta^2}} \frac{T_{m'}(\theta/A')}{\sqrt{A'^2 - \theta^2}}\, d\theta \tag{40}$$

where $T_m(x) = \cos(m \arccos x)$ are Chebyshev polynomials, and the integration is extended over entire region where all under-integral functions are real. If $\mu \gg 1$, coupling of the multipoles can be neglected, and the series is reduced to a set of independent equations:

$$\Lambda_{m,j} Y_{m,j}(A) = -R_0(A) Y_{m,j}(A) + \int_0^\infty K_{m,m}(A, A') Y_{m,j}(A')\, dA' \tag{41}$$

where $\Lambda_{m,j} = \nu - m\mu$ is treated as an eigenvalue, and $j = 1, 2, ...$ are the eigenmode numbers. Their solutions are known as radial modes [3]. One can see again that the rigid mode $Y_{0,1}(A) = 1,\ \Lambda_{0,1} = 0$ is an exact solution of Eq. (41) independently on distribution function. Other modes will be examined numerically.

5.1 Boxcar bunch

Several e.v. and e.f. of the boxcar bunch (17) are presented in Table 1 and Fig. 6. They can be found also by using of exact solutions obtained in Section 3. Corresponding values are given in Table 1 as a rational fraction in round brackets, and order of used Legendre polynomial is placed in square brackets. It is seen that, at any m, successive solutions are born by the

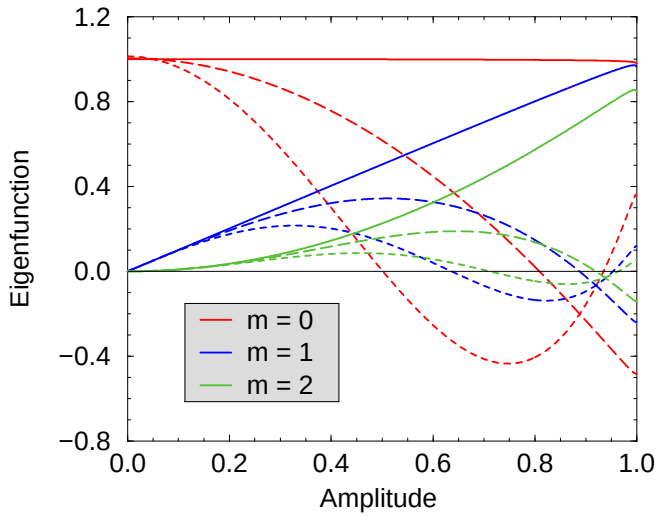

Figure 6: Eigenfunctions of the boxcar bunch (uncoupled multipoles approach). Three e.f. are presented for each multipole.

Table 1: Eigenvalues of the boxcar bunch

$m \downarrow j \rightarrow$	1	2	3
0	-0.013 (0) [0]	-0.754 (-3/4) [2]	-0.861 (-55/64) [4]
± 1	-0.509 (-1/2) [1]	-0.815 (-13/16) [3]	-0.884 (-113/128) [5]
± 2	-0.634 (-5/8) [2]	-0.846 (-27/32) [4]	-0.899 (-919/1024) [6]

polynomials of order $n = |m|$, $|m| + 2$, etc. At $m = 0$, eigenfunctions obtained by Fourier expansion of the exact solutions are

$$Y_{0,1} = 1, \qquad Y_{0,2} = 1 - \frac{3A^2}{2}, \qquad Y_{0,3} = 1 - 5A^2 + \frac{35A^4}{8}, \quad ...$$

being in a good agreement with numerical results, too. Similar situation is observed at dipole ($|m| = 1$) and higher oscillations.

5.2 Parabolic bunch

In contrast with the boxcar, parabolic model (32) bring the tune spread which is a key point for the Landau damping. As it is noted above, it should

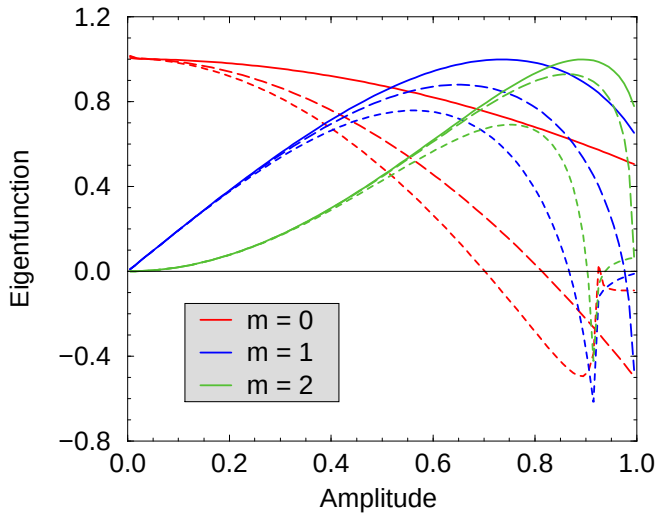

Figure 7: Modified e.f. of parabolic bunch (3 e.f. for each multipole).

appear as a irregularity of corresponding eigenfunctions. As it is shown in Fig. 7, this effect is observed at all radial modes other than lowest one, at $m = 0, 1, 2,$ (higher multipoles are not investigated). Corresponding "unstable" e.v. are:

$$\Lambda_{0,1} = 0, \qquad \Lambda_{1,1} = -0.422, \qquad \Lambda_{2,1} = -0.482.$$

All other investigated modes form a continuous spectrum at $-1<\Lambda_{m,j}<-0.5$. Because most of the e.f. have a peculiarity, continuous combinations are presented in Fig. 7 (including the regular lowest modes):

$$\tilde{Y}_{m,j}(A) = [\,\Lambda_{m,j} + R_0(A)\,]\,Y_{m,j}(A) = \Big[\,\Lambda_{m,j} + 1 - \frac{A^2}{2}\,\Big]\,Y_{m,j}(A), \qquad (42)$$

Note that originally irregular functions have a break of derivative in this format.

5.3 "Super-parabolic" and Gaussian bunches

In contrast with previous, "super-parabolic" bunch (33) has no derivative abruption on the boundary. Probably because of this the rigid mode (0,1)

is the only regular solution of Eq. (41), whereas all other modes have peculiarities and form continuous spectrum at $-1 \leq \Lambda \leq -3/8$. Some of these modes are presented in left-hand Fig. 8 in the format like (42).

Very similar picture appears at Gaussian distribution (34)-(36). Some e.f. are plotted at right-hand Fig. 8 at $\sigma = 1/3$ when the continuous spectrum is located at $-1 \leq \Lambda \leq -0.274$.

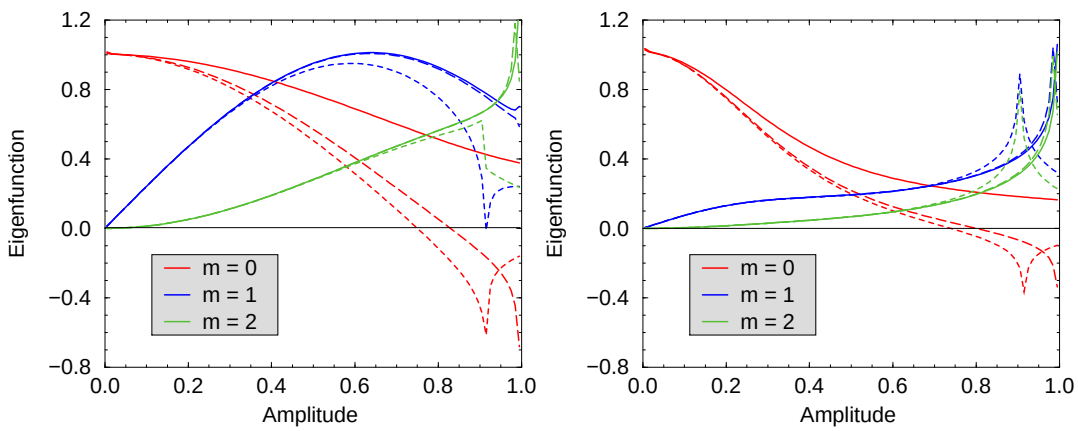

Figure 8: Modified e.v. of "super-parabolic" (left) and Gaussian (right) bunches.

6 Comparison and coupling of the models

The foregoing results were obtained at very extreme values of μ: either $\mu \ll 1$ or $\mu \gg 1$ (below: low/high-μ approximations). Correlation of this data is a subject in this section to fill the gap between the areas and to develop a reasonable picture at $\mu \sim 1$ (say, at $0.5 < \mu < 1.5$).

For boxcar bunch, overall picture is shown in Fig. 9 where red lines present two lower modes of Eq. (29)-(30) (formally referred to $\mu \ll 1$), and blue ones – e.v. of dipole and quadrupole modes $m = 1, 2$ in Eq. (41) (formally $\mu \gg 1$). Besides, exact solutions are presented by black lines being taken from Sec. 3 at $n = 1, 2$ (black and red lines coincide at $m = n = 1$). Trivial rigid mode is not included in all the cases. One can conclude that both models are in good

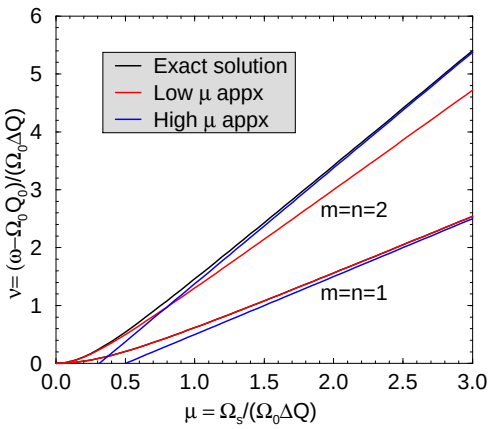

Figure 9: Eigenvalues of boxcar bunch: exact and 2 different approaches.

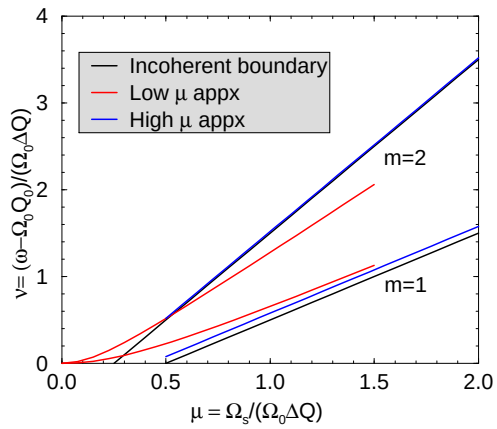

Figure 10: Approximate eigenvalues of parabolic bunch and incoherent boundary.

agreement with exact solution in region of interest to us, though low-μ and high-μ approximations work better at $\mu < 0.8$ and $\mu > 0.8$, respectively.

Similarly, numerical results are presented in Fig. 10 for parabolic bunch (32), using both approximations. Relative positions of red and blue lines in this picture are about the same as in Fig. 9, however, exact solution is unknown now. Instead of this, maximal incoherent betatron frequency is plotted being averaged on synchrotron phase. Its modulation by synchrotron frequency is taken into account, so equations of corresponding black lines are:

$$\nu = -0.5 + m\mu.$$

For each multipole, all incoherent frequencies are located below corresponding line; therefore, any eigenmode is stable (prone to Landau damping) if its e.v. is located below it as well. According to high-μ approximation, both modes shown in Fig. 10 by blue lines are unstable, whereas low-μ approximation predicts stability of 2nd mode at $\mu > 0.5$ (red line). However, last statement should be rejected because this approach is certainly worse at higher μ. It allows to establish the boundary between low/high-μ approximation as $\mu \simeq 0.5$ – a result which is not very distinctive from the boxcar case.

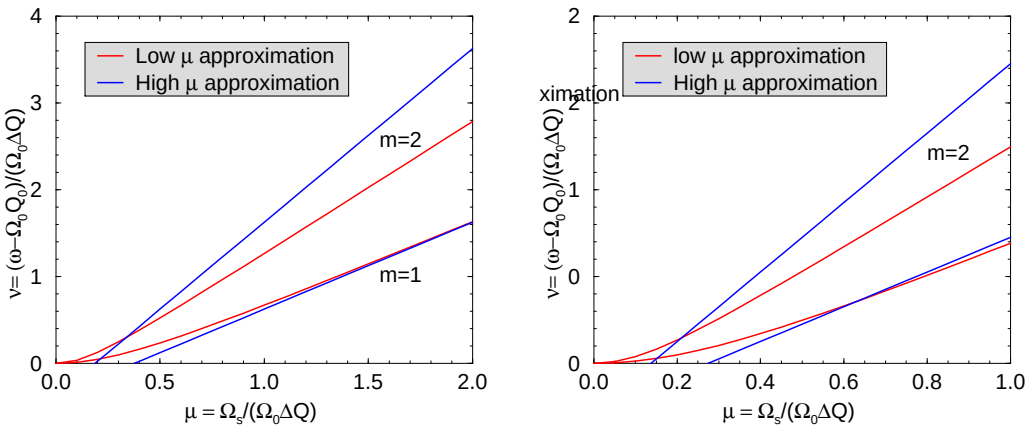

Figure 11: Eigenfunctions of "super-parabolic" (left) and Gaussian (right) bunches. The blue lines mark incoherent boundaries, too.

Eigenvalues of the super-parabolic and truncated Gaussian bunches (33)-(34) are summarized in Fig. 11. High-μ approximation predicts that all modes, except of rigid, are stable in these cases forming continuous spectra in the ranges

$$\nu < -0.375 + m\mu \qquad \text{or} \qquad \nu < -0.274 + m\mu$$

Blue lines in Fig. 11 are highest e.v. of the spectra coinciding with incoherent boundaries. Low-μ approximation presented here by red lines asserts that these modes are stable at $\mu \ll 1$. However, they demonstrate relatively strong growth on the bunch tails at $\mu >\sim 0.1$, and very strong (possibly infinite) growth at $\mu >\sim 0.5$ (see Fig. 3-5). Taking into account that similar behavior is a manifestation of Landau damping, one can propose the following conditions of stability:

m	1	2
Super-parabolic	$\mu >\sim 1.5$	$\mu >\sim 0.4$
Gaussian	$\mu >\sim 0.6$	$\mu >\sim 0.2$

The higher modes are all the more stable.

7 Conclusion

Transverse eigenfunctions and eigenfrequencies of a bunched beam are investigated in this article at space charge dominated beam coupling impedance, that is at relatively slight wake field. Synchrotron oscillations are taken into account at any relation of synchrotron frequency to space charge tune shift. It is shown that tune spread produced by the space charge, in combination with synchrotron oscillations, brings a powerful Landau damping which suppresses almost all transverse modes. The only mode which is never prone to this effect is so called rigid one which does not depend on synchrotron oscillations at all. In simplest case (no chromaticity), the rigid mode appears as transverse oscillations of the bunch as a whole (without bend or rotation), but a traveling wave runs over the bunch additionally at non-zero chromaticity. Other modes are suppressed at all if synchrotron frequency about exceeds space charge tune shift, and the distribution function has no abrupt boundaries. At the lower synchrotron frequency, several modes other the the rigid one can overcome Landau damping that is they are potentially unstable. In particular, for truncated Gaussian bunch, dipole mode may be unstable at $\Omega_s <\sim 0.6\,\Omega_0\Delta Q(0)$, quadrupole one – at $\Omega_s <\sim 0.2\,\Omega_0\Delta Q(0)$, etc. A distinguish characteristic of similar modes is a small global dipole moment (zero without chromaticity), and therefore relatively weak long-term wake field expected.

Obtained eigenfunctions can be used for calculation of wake field which produces a small additions to the eigenfrequencies, including instability growth rate. Global beam structure is essential at these calculations, determining characteristics of the collective modes. Detailed investigation of the collective motion based on the rigid modes of the bunches is presented in Ref. [10]. In particular, it is shown that resistive wall instability growth rate can reach 3000/sec in the Fermilab Recycler in frames of Project X, and 27 MHz damper or chromaticity about -7 are required to suppress it. Doubtless, other potentially unstable modes are not so dangerous because of relatively low integral dipole moment of any bunch; however, these investigations are beyond the scope of presented article.

References

[1] C. Pellegrini, Nuovo Cimento A64, 447 (1969).

[2] M. Sands, SLAC TN-69-8 (1969).

[3] F. Sacherer, CERN-SI-BR-72-5 (1972).

[4] V. Balbekov, Sov. Phys. Tech. Phys., Vol.21, No.7, 837 (1976).

[5] M. Blaskiewicz, Phys. Rev. ST Accel. Beams 1, 044201 (1998).

[6] A. Burov, Phys. Rev. ST Accel. Beams 12, 044202 (2009).

[7] A. Chao *Physics of Collective Beam Instabilities in High Energy Accelerators*, J. Wiley & Sons, Inc., NY, p. 172 (1993).

[8] V. Balbekov, Fermilab-FN-0783-AD (2006).

[9] L. Landau, J. Phys. USSR, 10, 25 (1946).

[10] V. Balbekov, Fermilab-TM-2372-AD (2007).